1963

A Technique for Measuring the Electrical Conductivity of Moving Conductors

Joseph Norwood
College of William & Mary - Arts & Sciences

A TECHNIQUE FOR MEASURING THE ELECTRICAL CONDUCTIVITY OF MOVING CONDUCTORS

A Thesis

Presented to

The Faculty of the Department of Physics

The College of William and Mary in Virginia

In Partial Fulfillment

Of the Requirements for the Degree of

Master of Arts

By

Joseph Norwood, Jr.

A TECHNIQUE FOR MEASURING THE ELECTRICAL CONDUCTIVITY OF MOVING CONDUCTORS

A Thesis

Presented to

The Faculty of the Department of Physics

The College of William and Mary in Virginia

In Partial Fulfillment

Of the Requirements for the Degree of

Master of Arts

By

Joseph Norwood, Jr.

APPROVAL SHEET

This thesis is submitted in partial fulfillment of

the requirements for the degree of

Master of Arts

Joseph Norwood, Jr.
Author

Approved, August 1963:

Frederic R. Crownfield, Jr.
Frederic R. Crownfield, Jr.

Melvin A. Pittman
Melvin A. Pittman

James D. Lawrence, Jr.
James D. Lawrence, Jr.

copy 2

ACKNOWLEDGMENTS

The author wishes to acknowledge his appreciation to Professor F. R. Crownfield, Jr. for his support and criticism through the preparation of this thesis. The author also wishes to express his indebtedness to Dr. Karlheinz Thom of the National Aeronautics and Space Administration for the concepts from which this work was developed and to Dr. G. Oertel and R. Costen for their valuable suggestions. The writer would also like to express his thanks to Mr. M. D. Williams for his help in conducting the experiment and to Mrs. N. A. Bartlett for her help in reducing the data.

TABLE OF CONTENTS

	Page
ACKNOWLEDGMENTS	iii
LIST OF FIGURES	v
ABSTRACT	vi
INTRODUCTION	2
Chapter	
I. THEORY OF THE CONDUCTIVITY PROBE	5
II. EXPERIMENTAL APPARATUS	10
III. EXPERIMENTAL RESULTS	16
IV. COMPARISON OF THEORY AND EXPERIMENT	28
V. CONCLUSIONS	30
BIBLIOGRAPHY	31
VITA	32

LIST OF FIGURES

Figure		Page
1.	Cross-section view of the Probe	11
2.	The Magnetic Probes	12
3.	The Experimental Layout	13
4.	Pictorial Diagram of the Data Recording System	15
5.	Typical Signal Oscillograms	17
6.	Semilog Plot of Trace Decay	19
7.	Stainless Steel, L_o = 4.5 mm	20
8.	Aluminum, L_o = 4.5 mm	21
9.	Stainless Steel, L_o = 1.57 cm	22
10.	Aluminum, L_o = 1.57 cm	23
11.	Stainless Steel, L_o = 3 cm	25
12.	Aluminum, L_o = 3 cm	26
13.	Calibration for High Magnetic Reynolds Numbers	29

ABSTRACT

A simple one-dimensional theory is presented which demonstrates the possibility of measuring the electrical conductivity of a moving conductor by measuring the decay time of the transient part of the eddy current induced when the conductor moves into a steady magnetic field. In the limit of large magnetic Reynolds numbers the conductivity depends only on the velocity of the sample and not on the geometry. Experiments are described which are in good agreement with theory up to magnetic Reynolds numbers of about seven. For higher magnetic Reynolds numbers the one-dimensional theory breaks down; however, the consistency of the data is such that a calibration may be made.

A TECHNIQUE FOR MEASURING THE ELECTRICAL CONDUCTIVITY OF MOVING CONDUCTORS

INTRODUCTION

Measurements of the electrical conductivity of moving conductors have been performed by several workers in the past few years, notably on steady plasma flows and on the ionized boundary layer encountered by reentering space vehicles.

In 1960 a method was suggested by Gourdine for measuring simultaneously the local electrical conductivity and velocity in a steady plasma flow.[1] The technique utilizes an exciter coil placed equidistant from two sensor coils. When a conductor flows through the three coils and the exciter coil is energized from an a-c source, a difference in amplitude and a phase shift may be measured between the outputs from the two sensors. The measurement of these two quantities allows the calculation of the velocity and conductivity of the flow.

Another device has been developed by Fuhs and others at Space Technology Laboratories which is capable of measuring the integral over space of σuB.[2] Physically this device consists of a U-shaped magnet which has its poles flush with the skin of the reentry vehicle whose boundary layer is to be analyzed. The magnet is energized by

---

[1]Gourdine, Meredith C., A Technique for Making Local Measurements of the Conductivity and Velocity of a Plasmajet, Plasmadyne Corp., Report No. PLR-71. June 22, 1960.

[2]Fuhs, Allen E., Development of a Device for Measuring Electrical Conductivity of Ionized Air During Reentry, Space Technology Laboratories TR-60-0000-09256. ASTIA AD 252-220. Sept. 20, 1960.

a coil powered from an a-c source and there is a sensor coil located between the magnet poles adjacent to the missile skin. The emf induced in this coil is used to compute $\int \sigma u B^2 d\tau$. The assumption is made in the theory that the induced magnetic field is much smaller than the applied one. This is shown to be the equivalent to the requirement that magnetic Reynold's number, $\sigma \mu_o u L$, where L is a characteristic length, be much smaller than unity.

The only attempt (insofar as the author has been able to find) to deal with the conductivity of a transient flow such as occurs in shock tubes or plasma guns was made by Lin, Resler, and Kantrowitz.[3] They were interested in measuring the electrical conductivity of the plasma produced behind a shock wave in a cylindrical shock tube. To do this, a d-c coil was placed over the tube with a sensor coil a few centimeters upstream from it. As the slug of conductive material passed into the field induced currents caused a change of flux in the sensor coil.

The theory of this device utilizes the cylindrical symmetry to write integral equations describing the voltage V and the integral of the voltage Φ as a function of the axial position of the front of the slug and the axial distribution of conductivity. The impulse function

$$g(x) = \int_o^R F(x,r)\, B_r(x,r)\, dr$$

---

[3]Lin, S. C., Resler, E. L., and Kantrowitz, Arthur, Electrical Conductivity of Highly Ionized Argon Produced by Shock Waves, J. Appl. Phys., vol. 26, No. 1, Jan. 1955.

where $F(x,r)$ is the flux through the sensor coil due to a unit current ring of radius r and distance from the sensor, x, is evaluated by calibrating the device with a moving metallic rod or slug. The dependence of the voltage pulse shape on the axial variation of conductivity is also calibrated.

The present investigation also involves an analysis of the transient part of the induced field as does the Lin, Rosler, and Kantrowitz technique. Unlike any of the investigations cited above, the model used shows no strong dependence on geometry. Since the model is easily solved using separation of variables, differential equation techniques seem more appropriate than the integral equation approach of Lin, Rosler, and Kantrowitz.

When a moving conductor penetrates a magnetic field eddy currents are induced which, by Lenz's law, tend to exclude the field from the conductor. The field is distorted, begins to diffuse into the conductor, and finally approaches a steady state. The time required for this equilibrium state to be attained may be expected to depend on the conductivity of the material into which the field is diffusing. In the present experiments relaxation time is recorded by means of a probe coil placed in the magnetic field to monitor the local rate of change of the magnetic flux density. The decay time of the probe signal as displayed on an oscilloscope can then be used to measure the electrical conductivity of the sample. Note, however, that the length, l, of the sample must be such that the transit time (l/v) is large compared to the decay time to be measured; that is, the sample must appear to be semi-infinite.

CHAPTER I

THEORY OF THE CONDUCTIVITY PROBE

The governing equations for the problem three of Maxwell's equations

$$\nabla \times \vec{B} = \mu_o \vec{J} + \epsilon_o \mu_o \frac{\partial \vec{E}}{\partial t} \tag{1}$$

$$\nabla \times \vec{E} = - \frac{\partial \vec{B}}{\partial t} \tag{2}$$

$$\nabla \cdot \vec{B} = 0 \tag{3}$$

and Ohm's law for moving media

$$\vec{J} = \sigma \left(\vec{E} + \vec{v} \times \vec{B} \right) \tag{4}$$

Combining equations (1) and (4) one obtains for the magnetic induction in a moving conductor

$$\nabla \times \vec{B} = \sigma \mu_o \left(\vec{E} + \vec{v} \times \vec{B} \right) + \epsilon_o \mu_o \frac{\partial \vec{E}}{\partial t} \tag{5}$$

Taking the curl of this equation and employing the vector identifies[4]

$$\nabla \times \nabla \times \vec{B} = \nabla \left(\nabla \cdot \vec{B} \right) - \nabla^2 \vec{B}$$

$$\nabla \times \left(\vec{v} \times \vec{B} \right) = \vec{v} \left(\nabla \cdot \vec{B} \right) + \left(\vec{B} \cdot \nabla \right) \vec{v} - \vec{B} \left(\nabla \cdot \vec{v} \right) - \left(\vec{v} \cdot \nabla \right) \vec{B}$$

one obtains from equations (2) and (3), assuming $\vec{J}$ constant

$$\nabla^2 \vec{B} = \sigma \mu_o \left\{ \frac{\partial \vec{B}}{\partial t} + \left(\vec{v} \cdot \nabla \right) \vec{B} \right\} + \epsilon_o \mu_o \frac{\partial^2 \vec{B}}{\partial t^2} \tag{6}$$

---

[4] G. E. Hay, Vector and Tensor Analysis, Dover Publications, Inc., New York, 1953, p. 117.

Since the separation constants which appear in the solution of the differential equation lead to exponentially decaying terms for the time-dependence, one predicts that, after a long enough time, only the lowest mode in the Fourier series will be of importance. The "decay constant" or 1/e-folding time of this term is easily obtained, and involves μ_o, σ, L_o, and v. It thus provides the desired relation between σ and a measurable quantity, the decay constant.

Equation (7) becomes in one-dimension

$$\frac{\partial B}{\partial t} = - v \frac{\partial B}{\partial x} + \frac{1}{\sigma\mu_o} \frac{\partial^2 B}{\partial x^2} \tag{9}$$

The variable may be separated in equation (9) by the usual substitution

$$B(x,t) = T(t)\, X(x)$$

which gives

$$\frac{\dot{T}}{T} = - \frac{vX'}{X} + \frac{1}{\sigma\mu_o} \frac{X''}{X} = \alpha$$

where α is the separation constant. Looking first at the equation for the time-dependent part

$$\dot{T} = \alpha T \rightarrow T = e^{\alpha t}$$

Solutions which grow exponentially with time cannot be allowed since a stationary solution is anticipated as $t \rightarrow \infty$. Thus, $\alpha = 0$ or $-\beta$, where β is a positive real quantity. The solutions with $\alpha = 0$ lead to the steady-state solution which is not of interest here.

Note, however, that the ratio of the displacement current term to the term in the bracket is $\epsilon_0\omega/\sigma$, where ω is the reciprocal of the characteristic pulse width. Thus for typical metallic conductivities ($\sigma \sim 10^6$ mho/m) the displacement current term is negligible for all ω below the soft x-ray region, that is, for $1/\omega > 10^{-17}$ seconds.

$$\frac{\partial \vec{B}}{\partial t} = - (\vec{v} \cdot \nabla) \vec{B} + \frac{1}{\sigma\mu_0} \nabla^2 \vec{B} \qquad (7)$$

which has the form of a diffusion equation.

A two- or three-dimensional treatment of this problem is complicated by the fact that there is no such thing as a magnetic field with sharply defined boundaries; in fact, a field with only one nonzero component would be uniform over all space, and the moving conductor would never "enter" the field.

Instead of a realistic multidimensional model, it is proposed to solve the following one-dimensional idealization. Before the conductor enters, assume a magnetic field in the z-direction which is zero except for a region of width L_0 in the x-direction. In this region, the field has constant magnitude B_0 before the entry of the conductor. The differential equation in one dimension is solved for the magnetic field in this finite region of length L_0 under the assumption that the solution at $t = 0$ yields the magnetic field which was present before the entry of the conductor. This somewhat artificial assumption is equivalent to ignoring the transit of the leading edge of the conductor through the field, but allows one to expand the induced field in a Fourier series.

With $\alpha = -\beta$

$$\dot{T} + \beta T = 0 \rightarrow T = e^{-\beta t}$$

and

$$X'' - \sigma\mu_o v X' + \sigma\mu_o \beta X = 0$$

The solution of latter equation can be written in the form

$$X = e^{\sigma\mu_o v x/2}\left\{A_1 e^{\delta x} + A_2 e^{-\delta x}\right\}$$

where

$$\delta = \sqrt{\left(\frac{\sigma\mu_o v}{2}\right)^2 - \sigma\mu_o \beta}$$

In order that a nonzero solution exist only over a finite region of space ($0 \leq x \leq L_o$), as required by the one-dimensional model, X must be expressible as a Fourier series, that is, δ must be imaginary. This gives

$$\sigma\mu_o \beta > \left(\frac{\sigma\mu_2 v}{2}\right)^2$$

and

$$\sigma\mu_o \beta - \left(\frac{\sigma\mu_o v}{2}\right)^2 = \left(\frac{n\pi}{L_o}\right)^2$$

Thus β is given by

$$\beta = \frac{(2n\pi)^2 + R_m^2}{4\ \sigma\mu_o\ L_o^{\ 2}}$$

and $\beta = 1/\tau$, the 1/e folding time for the amplitude of B and $\partial B/\partial t$ is

$$\tau = \frac{4\,\sigma\mu_o\,L_o^2}{R_m^2 + (2\pi n)^2} \tag{10}$$

where R_m is the magnetic Reynolds number, $R_m = \sigma\mu_o\, v\, L_o$.[5]

For the case where $R_m \ll 2\pi n$, τ is dependent on the characteristic field dimension, L_o, but independent of the velocity

$$\tau \approx \frac{\sigma\mu_o\,L_o^2}{\pi^2 n^2} \tag{11}$$

This same result has been reached by Goldstein in connection with the problem of penetration of magnetic fields into incompressible plasmas.[6]

For the opposite extreme, $R_m \gg 2\pi n$, L_o drops out and τ goes like $1/v^2$

$$\tau \approx \frac{4}{\sigma\mu_o\,v^2} \tag{12}$$

In relating the theory to the experiments only the first term of the Fourier series will be taken ($n = 1$). This approximation is suggested by the fact that n is contained in β quadratically, and hence the higher modes damp out much more rapidly than the first. This decision is further supported by the fact that the oscilloscope traces are found experimentally to have an exponential decay; the sum of exponentials of different argument and amplitude would not be exponential.

---

[5] Cowling, T. G., Magnetohydrodynamics, Interscience Publishers, New York, 1957, p. 6.

[6] Goldstein, Melvin, The Penetration of Magnetic Fields in Incompressible Plasmas - Part I, PIBMRI-919-61 ASTIA AD No. 294494, Polytechnic Institute of Brooklyn Microwave Research Institute, Brooklyn, New York.

CHAPTER II

EXPERIMENTAL APPARATUS

The first magnetic probes were made by placing a 110 turn coil of 41 AWG copper magnet wire directly in front of a cylindrical Alnico magnet of 25 mm length and 4.5 mm diameter. A second coil, identical to the first, but wound in the opposite sense, was connected in series and located 7.6 cm from the first coil. This coil was intended to cancel induced effects due to possible external fields. The assembly of magnet and coils were cast in epoxy resin, and the resulting cylinder received a 5×10^{-2} mm coating of chemically deposited copper electrically connected to the braided sheaths of the two Microdot output cables. This was finally encased in an 8 mm pyrex tube with a flat end window in front of the probe coil. It was anticipated that this probe would be used to measure plasma conductivities in a coaxial plasma gun hence the electrostatic and induction shielding was deemed necessary.

Since the sample conductor must have the configuration of a plane sheet for comparison with the theory, it was reasoned that the coaxial plasma gun, at least in its present configuration, would not provide a suitable apparatus to test the technique.

Hence, a broad bladed propeller of 122 cm diameter with insertable tips, 20 cm by 5 cm, was used. A 200 hp variable frequency

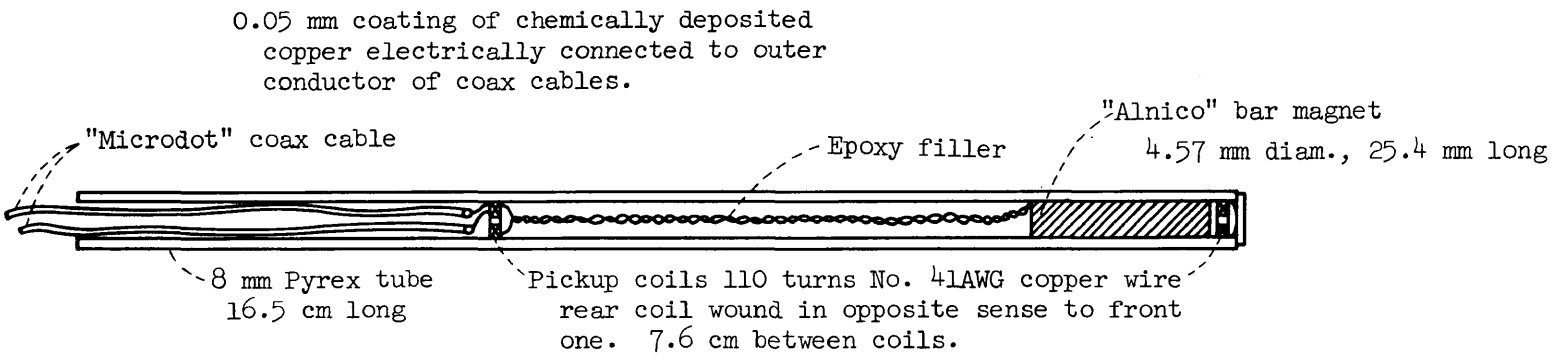

Scale: 1 = 1

Figure 1.- Cross-section view of the probe.

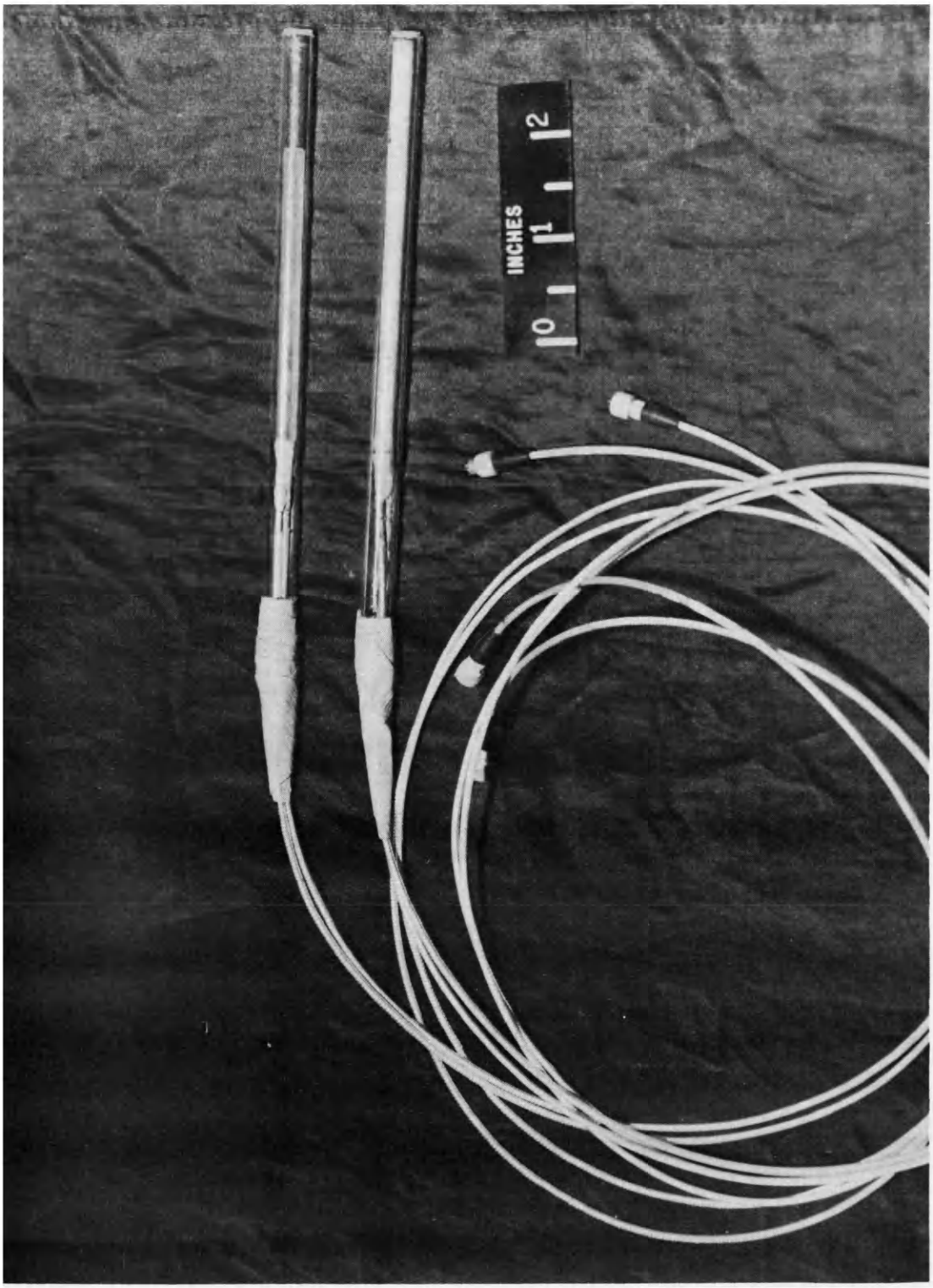

Figure 2.- The magnetic probes.

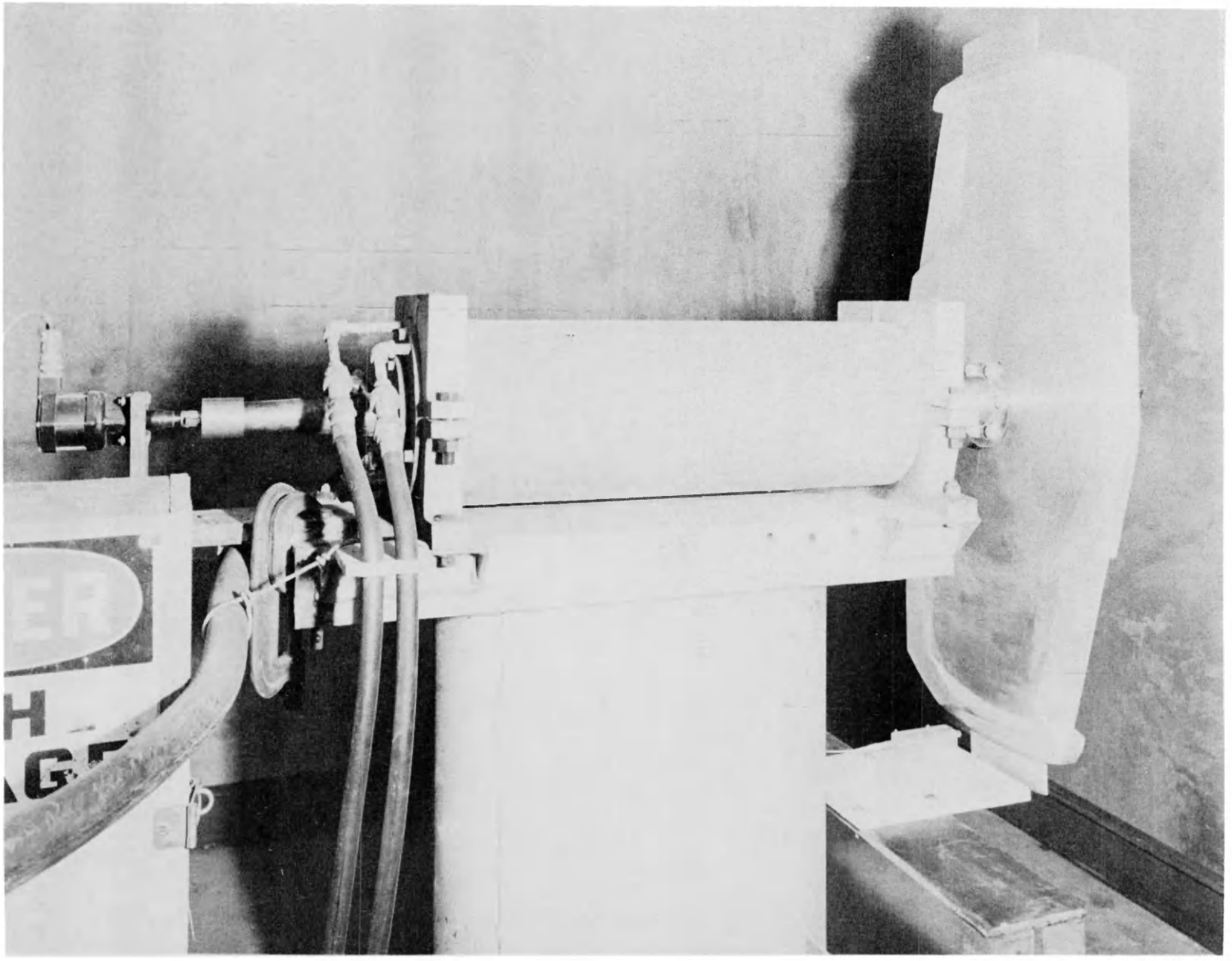

Figure 3.- The experimental layout.

motor was used to drive the propeller. The tips, which passed close to the probe and served as test samples, were of type 347 stainless steel and aluminum alloy 2024-T3, respectively. The electrical conductivity as obtained from manufacturer's data of 347 stainless steel is 1.25×10^6 mho/m; for aluminum, 2.27×10^7 mho/m. The motor could be regulated so that the velocity of the tips past the probe could be varied from 47 m/sec to 300 m/sec. The speed of the motor was measured with an aircraft-type tachometer which was calibrated against a General Radio Strobotac.

The probe coil was connected to a type L preamplifier in one channel of a Tektronix model 555 dual beam oscilloscope. The output signal of the plus gate of this channel was then used to trigger a Rutherford time-delay pulse generator, model A2, which triggered the horizontal sweep of the second channel of the oscilloscope.

The reason for this arrangement was that the signals caused by the action of the tips passing the probe varied in amplitude due to the difference in the tip conductivities. The first channel of the oscilloscope could be triggered by the larger of the two pulses (corresponding to the transit of the aluminum tip), and the trigger signal from the Rutherford time-delay pulse generator could be delayed by a time corresponding to a half-rotation of the propeller to delay the pulse corresponding to the stainless steel tip or by a time equivalent to a whole rotation to read data for the aluminum.

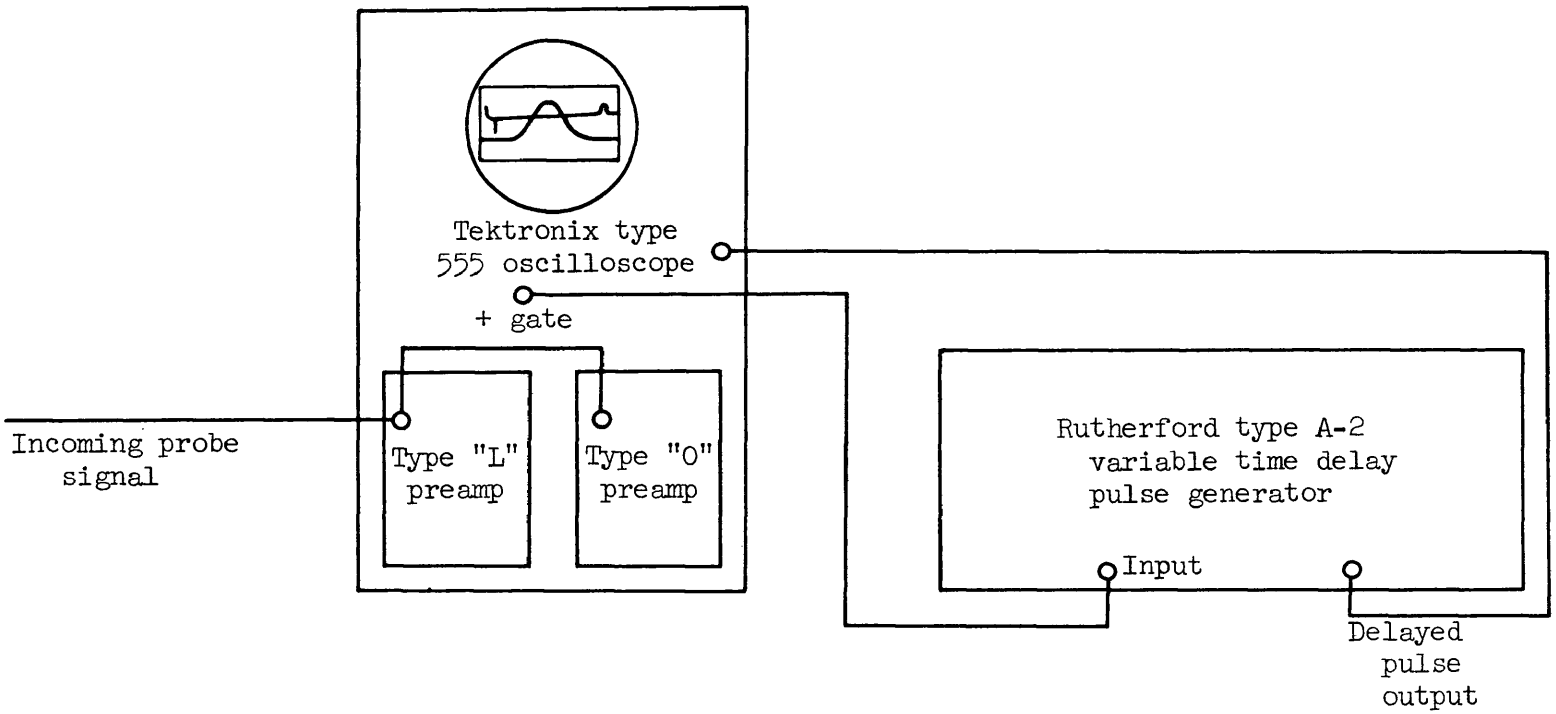

Figure 4.- Pictorial diagram of the data recording system.

CHAPTER III

EXPERIMENTAL RESULTS AND DISCUSSION

Typical signal traces are shown in figure 5. In the oscillogram at the top of the page the lower trace corresponds to the stainless steel sample entering the field. The time scale for this trace is 50 microseconds per large division. The top trace shows the pulses received in slightly more than a 180° rotation time for the propeller. The large pulse of the aluminum (which triggers the upper channel and the time delay pulse generator) is on the left and the pulse of the stainless steel is seen about two thirds way across the oscillogram. The time scale is two milliseconds per large division. The velocity of the stainless steel sample at the time that this oscillogram was taken was 133.5 meters per second. A similar oscillogram showing an aluminum pulse on the lower trace is seen at the bottom of figure 5. The dip of the trace below the zero line in each case is due to the fact that the sample traverses a weak field whose direction is opposite to that of the main field just before the main field is penetrated.

The decay time, τ, has been determined from these oscillograms by taking a point to the right of the peak which is on the exponentially decaying slope and measuring the horizontal distance which corresponds to the 1/e amplitude decay. The fact that the decay is purely exponential was checked by making semilog plots for a

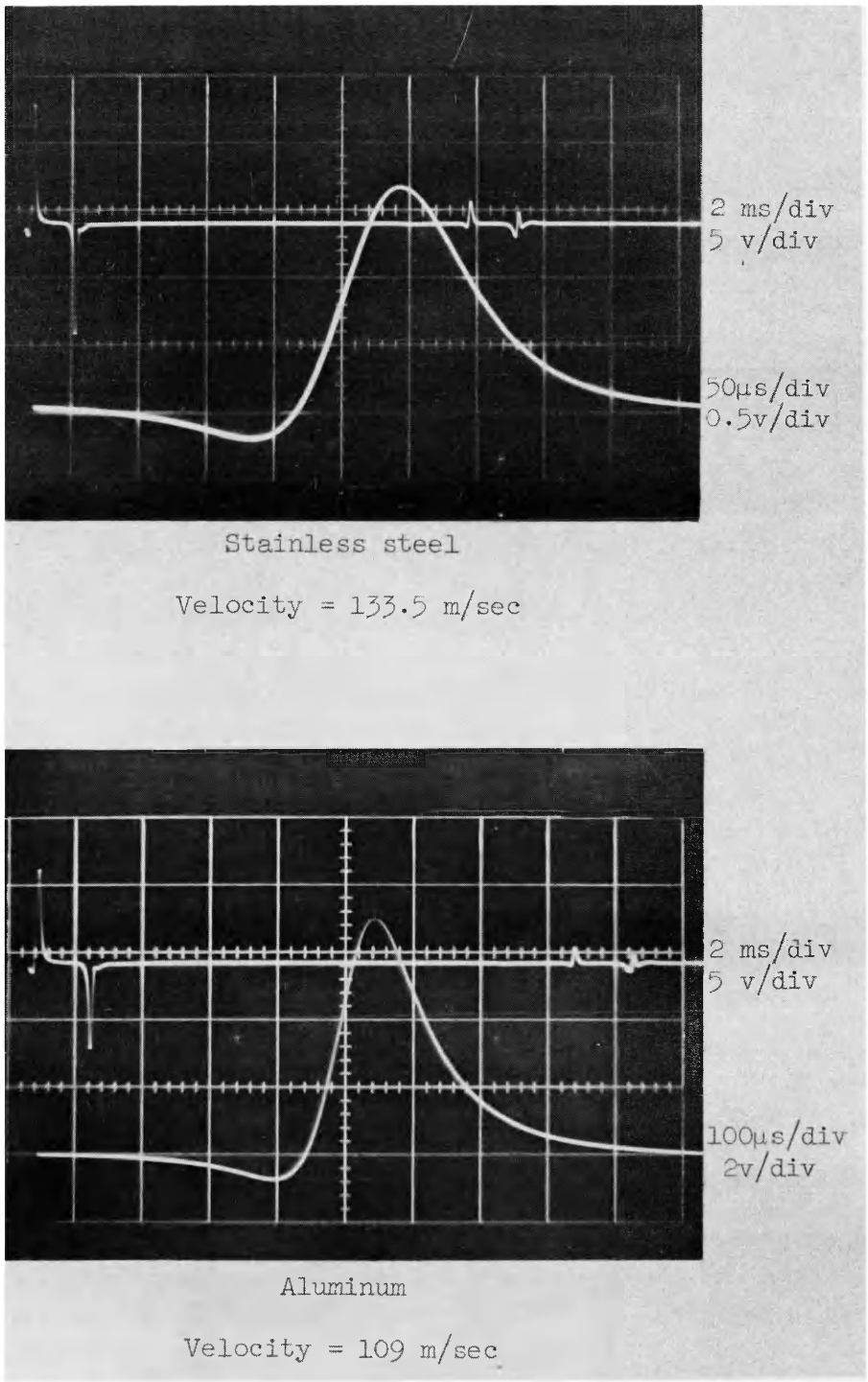

Figure 5.- Typical signal oscillograms.

representative sampling of the oscillograms; a typical example is shown in figure 6.

In figures 7 and 8 the decay time, τ, from equation (10) has been plotted as a function of velocity, v, and magnetic Reynolds number, R_m, using the values of conductivity quoted above and $L_o = 4.5$ mm, the diameter of the magnet pole face. On figures 7 and 8, respectively, one notes that the data are in considerable disagreement with the theoretical curves. This may be explained by the divergent nature of the magnetic field eminating from the probe magnet. The dimension, L_o, which has been taken to be 4.5 mm, the magnet diameter, should actually represent an average dimension of the B_o field in the conductor under investigation. In the case of a bar magnet, the pole-face diameter is obviously a poor approximation. Noting that the data on figure 7 are in the velocity independent region it seems reasonable that the value of L_o selected was too small and a larger value would result in good agreement. Consequently, equation (10) is solved for L_o to give

$$L_o = \sqrt{\frac{4\tau\pi^2}{\sigma\mu_o\,(4 - \sigma\mu_o v^2\tau)}} \qquad (13)$$

and the point $\tau = 3.4 \times 10^{-5}$, $v = 10^2$ is inserted to give a corrected value for L_o of 1.57 cm. The corrected value of L_o may be interpreted as the effective dimension of the field at a distance of 1.2 cm from the end of the magnet at which distance the moving conductor passed. Theoretical curves using the corrected value of L_o are compared with the data on figures 9 and 10. Note that this

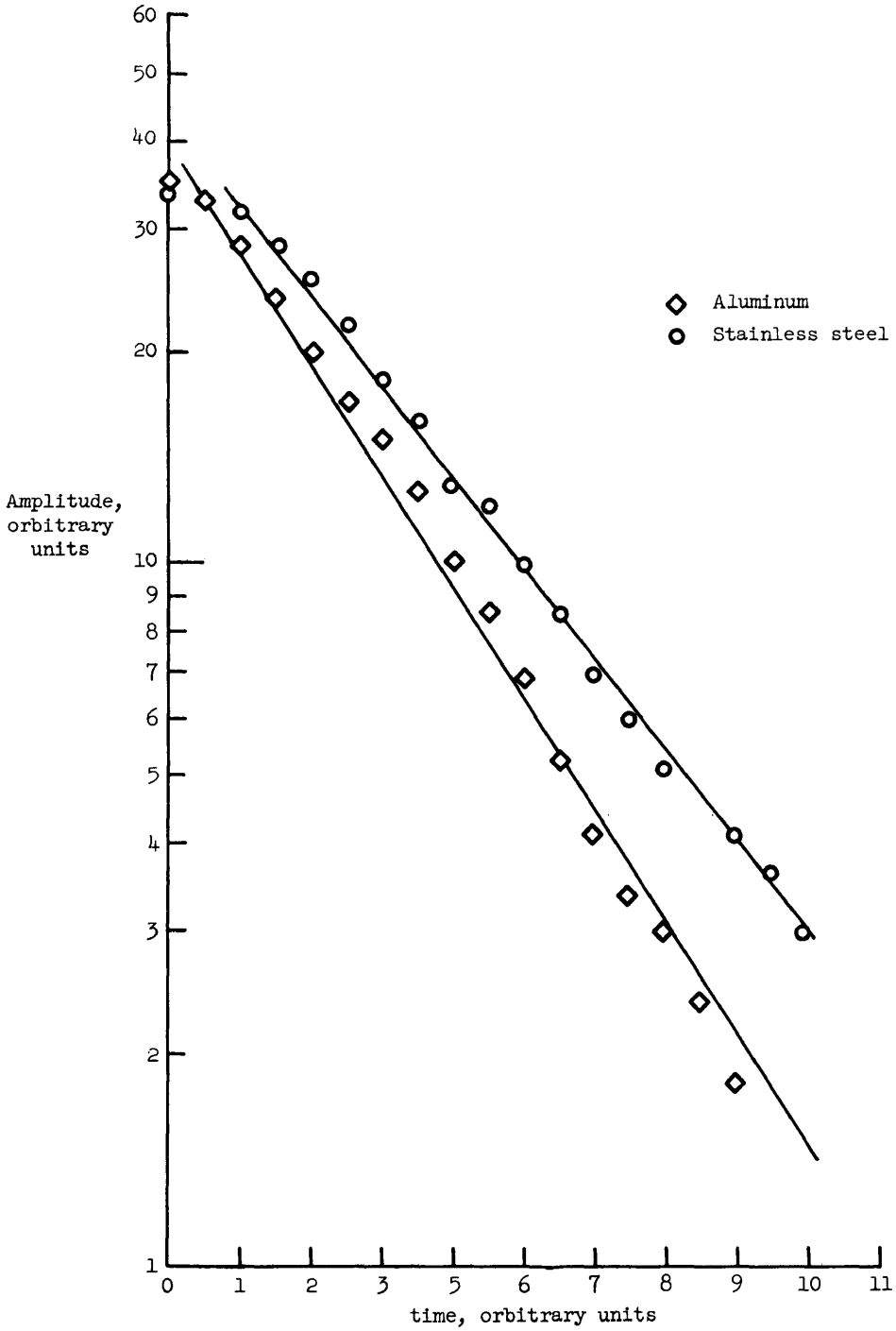

Figure 6.- Semilog plot of the decay of the two typical traces shown in figure 5.

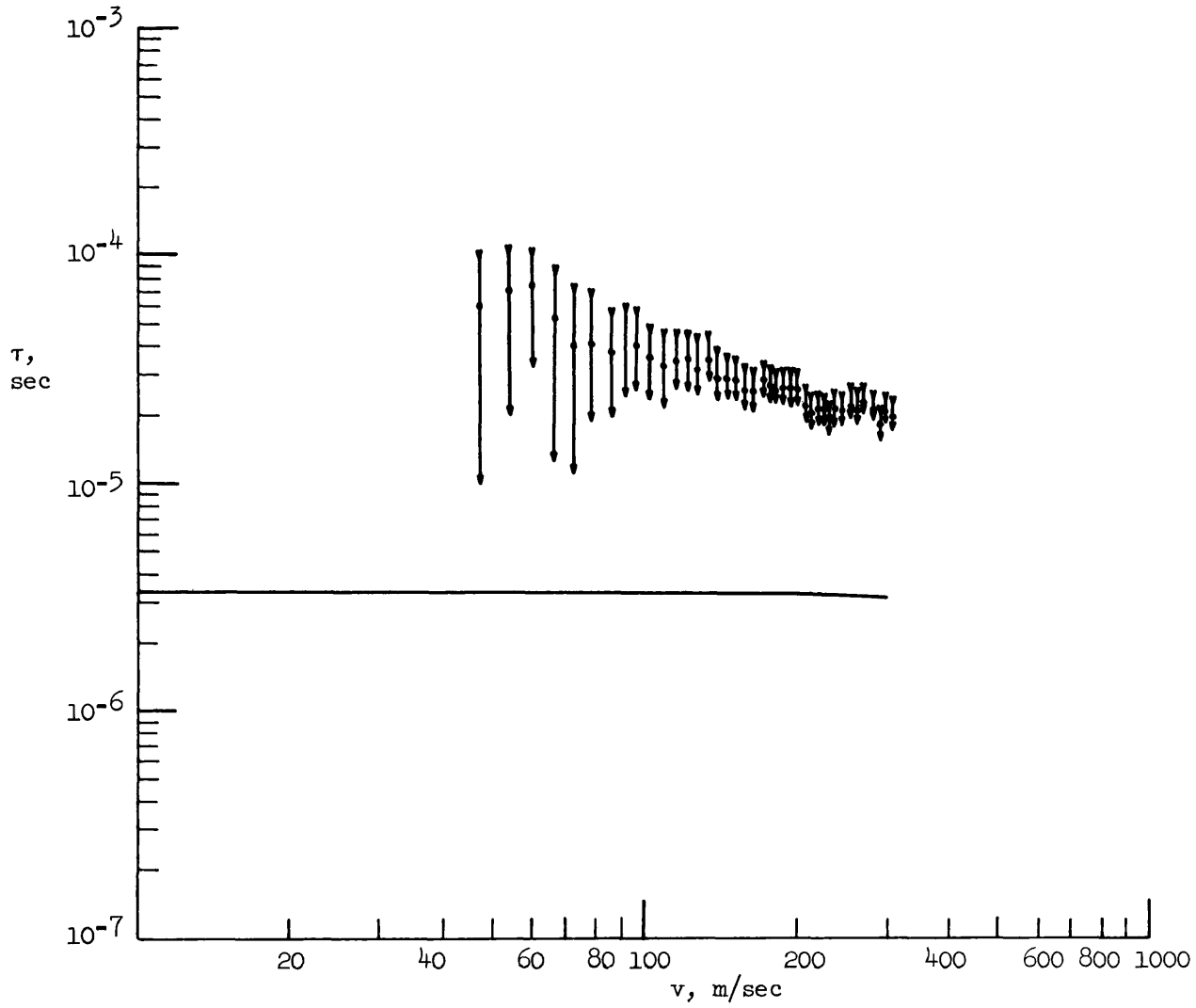

Figure 7.- Decay constant versus velocity and magnetic Reynold's number for stainless steel, L_o = 4.5 mm.

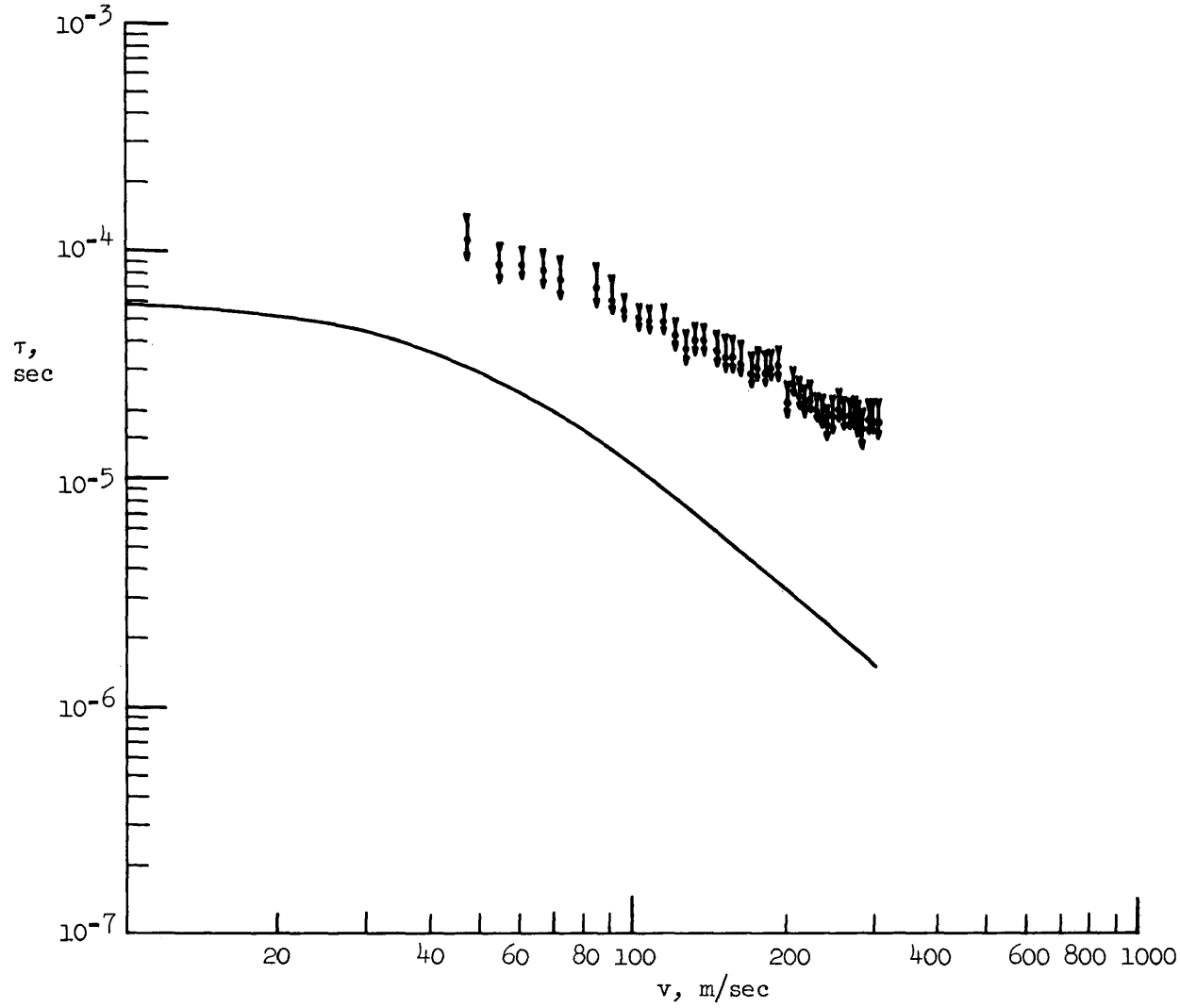

Figure 8.- Decay constant versus velocity and magnetic Reynold's number for aluminum, L_o = 4.5 mm.

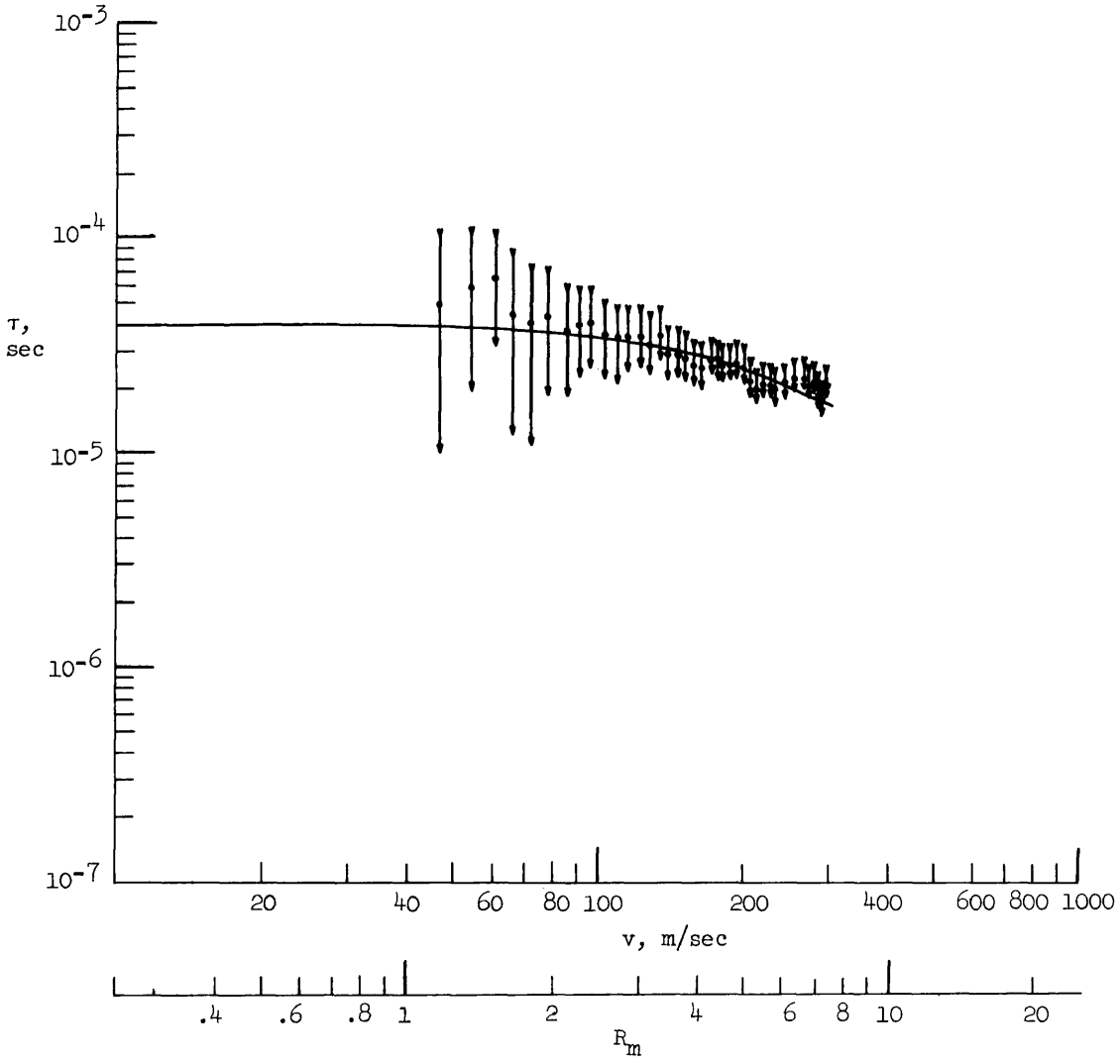

Figure 9.- Decay constant versus velocity and magnetic Reynold's number for stainless steel, L_o = 1.57 cm.

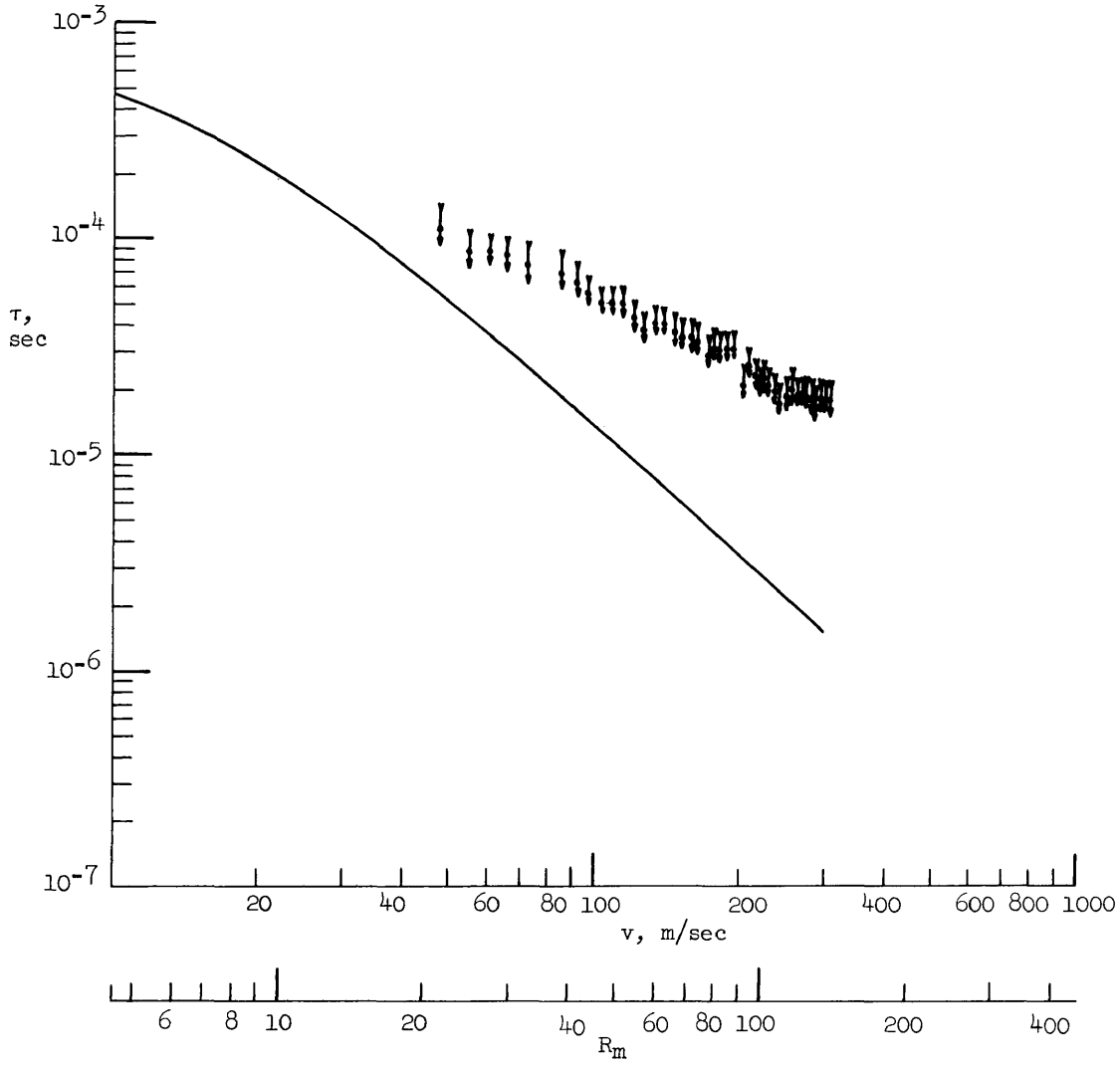

Figure 10.- Decay constant versus velocity and magnetic Reynold's number for aluminum, L_o = 1.57 cm.

correction has put the experimental data for stainless steel into good agreement with theory. The progressive deviation of the values for aluminum from the theoretical curve will be discussed in the next chapter.

The lengths of the error bars were dictated by two considerations. In the case of the stainless steel data the amplitudes of the traces from $v = 47$ meters per second up to a velocity of approximately 100 meters per second were comparable with the noise level (~ 150 microvolts). The height of the error bars for these cases were determined by use of the formula

$$\frac{V_{noise}}{V_{amplitude}} \times 100 = \text{percent error}$$

It was assumed that a reading error of 5 percent was reasonable for the rest of the points.

Several different probe geometries, distances of separation from the magnet to the sample, and angle between $\vec{v}$ and the long axis of the probe were tried. The results were quantitatively the same. More or less correction was made to L_o depending on how well the configuration approximated the one-dimensional model on which the theory was based. In figures 11 and 12 data are presented which was taken with a probe constructed using a 0.5 Weber/m^2 magnetron magnet with a pole face-diameter of 3 cm and a gap of 2.5 cm. A 100-turn coil was fastened onto one face with epoxy cement and the blades were allowed to pass between the poles.

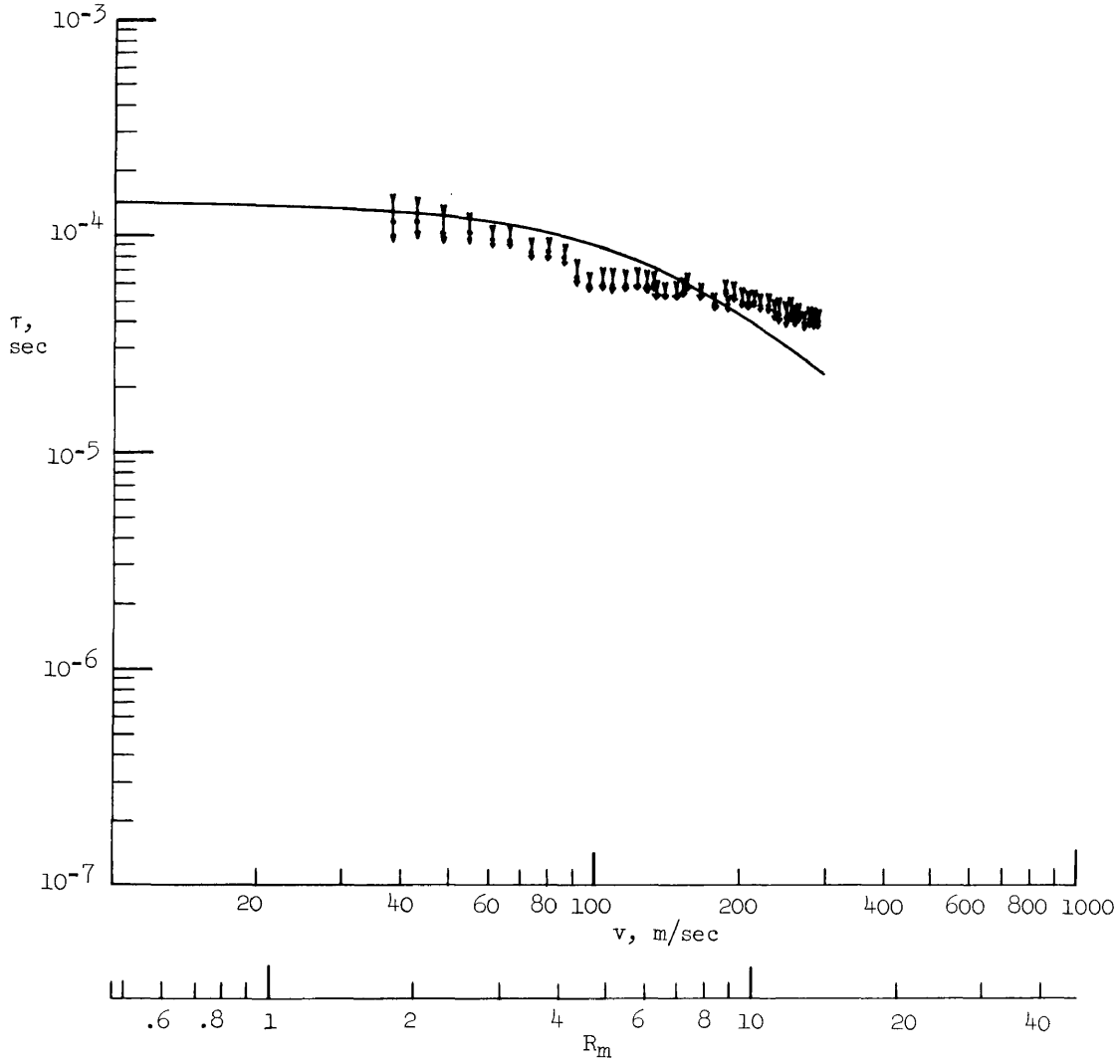

Figure 11.- Decay constant versus velocity and magnetic Reynold's number for stainless steel, L_o = 3 cm.

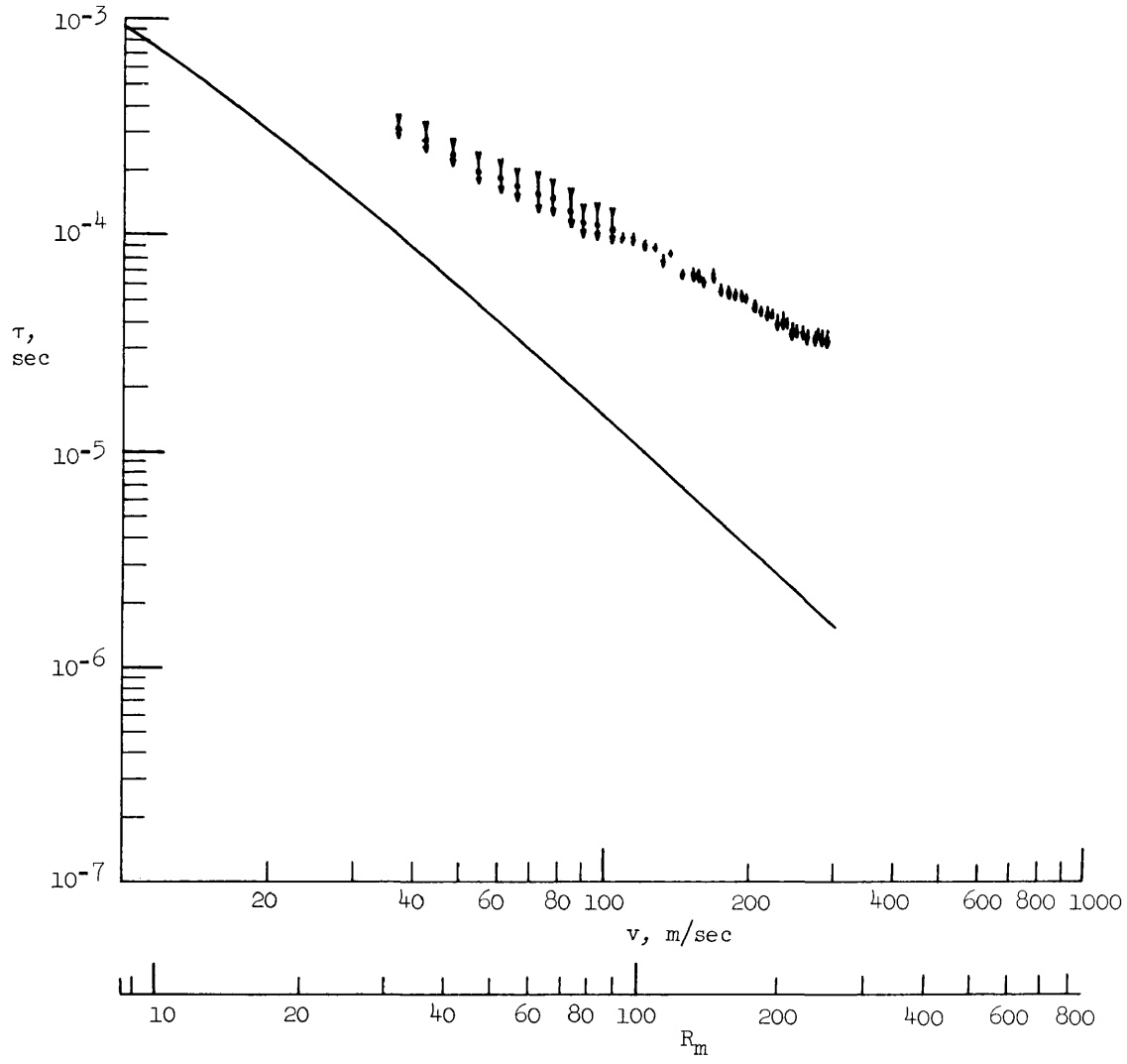

Figure 12.- Decay constant versus velocity and magnetic Reynold's number for aluminum, L_o = 3 cm.

In figures 11 and 12 the theoretical curves use $L_0 = 3$ cm, the pole-face diameter. From the fit obtained one may conclude that this configuration needs no correction for fringing. This is certainly a better approximation to the one-dimensional model. This probe was also capable of producing higher magnetic Reynolds numbers. The constancy of the sample velocity under the large impulse forces associated with this probe is demonstrated by the fact that the data seem to be compatable with that obtained from the smaller probes.

CHAPTER IV

COMPARISON OF THEORY AND EXPERIMENT

The reason for plotting the data as a function of magnetic Reynolds number is that R_m is a measure of the interaction of the field with the moving conductor. It is reasonable to expect that for large magnetic Reynolds numbers a marked deviation from one dimensionality will occur and the one-dimensional theory will break down.

Looking at figures 10 and 12, one notes that a straight line drawn through the data on these figures will be tangent to the knee of the curve, $R_m \approx 2\pi$. For $R_m < 2\pi$ rather good agreement between theory and experiment is obtained.

In order to determine whether the deviation of theory from experiment followed a consistant pattern for all of the data taken, the function

$$\eta = \frac{\tau_{measured} - \tau_{theoretical}}{\tau_{measured}}$$

was computed and is shown plotted in figure 13 as a function of magnetic Reynolds number. Note that all the points appear to fall on a common curve with very little scatter. Insofar as its use as a measuring device is concerned, the probe may thus be calibrated for the region $R_m > 2\pi$ where the theoretical model breaks down.

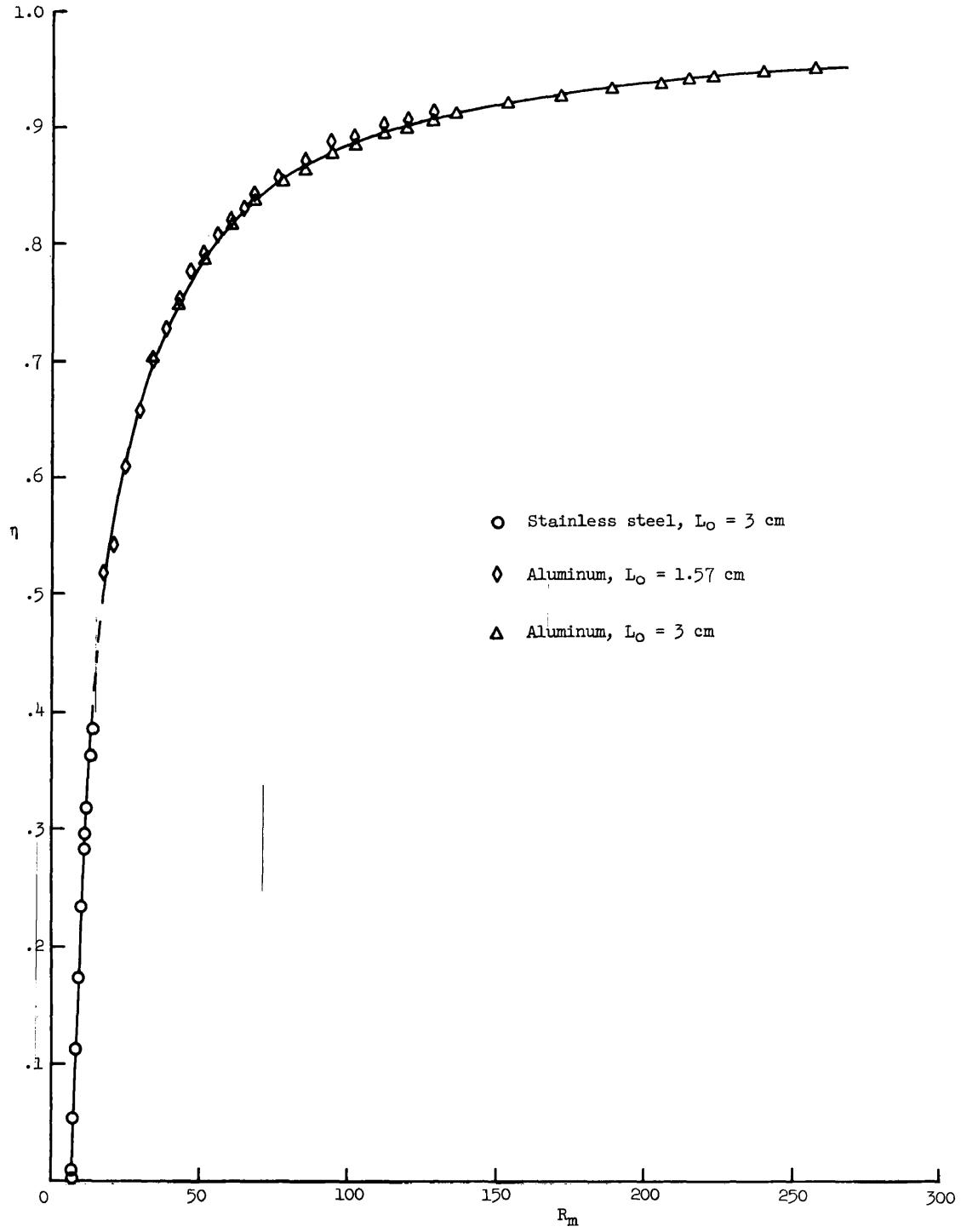

Figure 13.- Deviation function, η, versus magnetic Reynold's number to serve as a calibration for high magnetic Reynold's numbers.

CHAPTER V

CONCLUSIONS

The validity of the theory has been established up to the point where the increasing dynamic interaction of the field with the conductor causes the one-dimensional model to cease to apply. It was felt to be outside of the scope of the present work to try to formulate a multidimensional theory since such a problem would no longer have stationary boundaries and would be quite difficult to solve. The emphasis has rather been to investigate whether the deviation of the one-dimensional theory from the experimental data is of a systematic nature with respect to the strength of the field-conductor interaction. That this is true has been established.

The question of applicability of this probe must be answered in connection with a particular experiment. The use of this probe for determining the conductivity of plasmoids in flight is open to question because of the inherent nonuniformity of the plasma boundaries and because plasmoids always have a "frozen-in" magnetic field. It is felt, however, that the present approach to this technique reveals more in the way of information needed to assess its applicability to specific cases than would an integral equation approach to the multidimensional problem.

BIBLIOGRAPHY

Cowling, T. G., Magnetohydrodynamics. Interscience Publishers, Inc., New York. 1957. *(5)

Fuhs, Allen E., Development of a Device for Measuring Electrical Conductivity of Ionized Air During Reentry. *(2)

Goldstein, Melvin, The Penetration of Magnetic Fields in Incompressible Plasmas - Part I. PIBMRI-919-61, ASTIA AD No. 294494. *(6)

Gourdine, Meredith C., A Technique for Making Local Measurements of the Conductivity and Velocity of a Plasma Jet. Plasmadyne Corp. Report number PLR-71. June 22, 1960. *(1)

Hay, G. E., Vector and Tensor Analysis, Dover Publications, Inc., New York, 1953. *(4)

Landau, L. D., and Lifshitz, E. M., Electrodynamics of Continuous Media. Addison-Wesley Publishing Company, Inc. Reading, Mass. 1960. 45.

Lin, S. C., Resler, E. L., and Kantrowitz, Arthur, Electrical Conductivity of Highly Ionized Argon Produced by Shock Waves. J. Appl. Phys., vol. 26, No. 1. January, 1955. *(3)

*Numbers in parenthesis correspond to footnote numbers in the text.

VITA

Joseph Norwood, Jr.

Born in Baltimore, Maryland, September 27, 1935. Graduated from New Hanover High School in Wilmington, North Carolina, June 1953; A.A. in Engineering, Wilmington College, Wilmington, North Carolina, June 1955; B.S. in Physics, University of North Carolina, June 1958. In September 1961, the author entered the College of William and Mary as a M.A. candidate in Physics. The author has been employed by the National Aeronautics and Space Administration, Langley Research Center, Langley Station, Hampton, Virginia as an Aerospace Engineer from 1957 to the present.